Journal of
Synchrotron
Radiation

ISSN 0909-0495

Received 27 August 2007
Accepted 19 November 2007

Complex of human neutrophil elastase with 1/2SLPI

Masahiro Koizumi, Aiko Fujino, Kay Fukushima, Takashi Kamimura and Midori Takimoto-Kamimura*

Teijin Institute for Bio-medical Research, Asahigaoka, Hino, Tokyo 191-8512, Japan.
E-mail: m.kamimura@teijin.co.jp

SLPI (secretory leukocyte protease inhibitor) is a 107-residue non-glycosylated protease inhibitor, which inhibits a wide range of serine proteases, trypsin, chymotrypsin, neutrophil elastase, chymase and cathepsin G. X-ray crystallographic analyses have shown that SLPI comprises two separate domains of similar architecture [Grütter, Fendrich, Huber & Bode (1988), *EMBO J.* **7**, 345–351] and the C-terminal domain interacts with bovine α-chymotrypsin. In order to understand SLPI's multiple functions against various serine proteases, the complex HNE (human neutrophil elastase) has been co-crystallized with 1/2SLPI (recombinant C-terminal domain of SLPI; Arg58–Ala107), which has a biological activity similar to full SLPI. The 1/2SLPI and HNE complex structure was solved at 1.7 Å resolution, and compared with the interaction mechanism of elafin, which is a specific inhibitor of elastase. It was found that P1 Leu72i and six hydrogen bonds between the main chains in the primary contact region have sufficient ability to inhibit HNE and PPE (porcine pancreatic elastase), and P5 Tyr68i is important in increasing the selectivity of 1/2SLPI against HNE. The mechanisms of the functions of SLPI are relatively unknown, but the current study could help understand the selectivity of SLPI against HNE and PPE.

Keywords: elastase inhibitor; crystal structure; SLPI.

1. Introduction

The SLPI (secretory leukocyte protease inhibitor) similar domain motif is present in several other secreted proteins called the WAP four-disulfide core (WFDC) domain family. Elafin is one of these proteins (Wiedow *et al.*, 1990, 1991; Zani *et al.*, 2004), a 57-residue protease inhibitor that is a potent and specific strong inhibitor of PPE and HLE (human leukocyte elastase). However, the SLPI C-terminal domain inhibits HNE but inhibits PPE weakly (Masuda *et al.*, 1994).

The X-ray structure shows that elafin inhibits PPE in a similar way as the SLPI C-terminal domain (Tsunemi *et al.*, 1996). How are these differences in selectivity against serine proteases between SLPI and elafin caused? Elafin and SLPI have multiple important roles both in normal homeostasis and at the site of inflammation. These include anti-protease and anti-microbial activity as well as modulation of the response to LPS stimulation. Both are members of larger families of proteins secreted predominantly at mucosal sites and are modulated under multiple pathological conditions, and control the conditioning of the innate immune system. The functions of SLPIs are still unclear (Williams *et al.*, 2006). We report here the details of their interactions with 1/2SLPI and HNE and describe the comparison with elafin:PPE complexes (Tsunemi *et al.*, 1996).

2. Materials and methods

2.1. Crystallization

1/2SLPI was designed as a half-size SLPI, which corresponds to the C-terminal domain and is expressed in *E. coli*. HNE was purchased from Elastin Products Company (Pacific, MO, USA). To obtain the HNE and 1/2SLPI complex, the mixed sample was dialyzed against 20 m*M* Na-acetate buffer (pH 5.0) using Slide-A-Lyzer (5000 Mw) to remove excess 1/2SLPI molecules. The crystallization was performed using the sitting-drop vapor-diffusion method at 293 K. Jena Bioscience Screening kits were used for the initial condition search. The crystals appeared from 2.0 *M* Na-formate at pH 4.5 in a few days and grew to a typical crystal size of 0.4 × 0.2 × 0.01 mm in one week.

2.2. Data collection and processing

Data collection was carried out under nitrogen stream at 100 K using *Quantum315* at beamline BL41XU of SPring-8. Paraton was chosen as a cryoprotectant and added to the crystallization condition 40%(*v*/*v*). The crystal belongs to $P4_22_12$ with unit-cell constants of $a = b = 106.64$ Å, $c = 55.12$ Å. The data set was processed using *Crystal Clear 1.3.5*. The initial phase was determined by molecular replacement with only HNE using *MOLREP* (CCP4.6.01 suite).

2.3. Refinements

Refinements were carried out using *REFMAC5* (CCP4.6.01 suite). After several cycles of map fitting of the HNE protein structure, we identified the electron density corresponding to 1/2SLPI. The 1/2SLPI model was constructed using *QUANTA2000* (MSI) with reference to the elafin (Tsunemi *et al.*, 1996) main-chain trace. The crystallographic data are shown in Table 1.

Table 1
Crystallographic data and refinement statistics of the HNE with 1/2SLPI complex.

Values in parentheses are for the outer shell (1.74–1.70 Å).

Data collection	
Space group	$P4_22_12$
Cell dimensions (Å)	$a = b = 106.64$, $c = 55.12$
Resolution (Å)	38.32–1.70 (1.74–1.70)
Total observations	419005
No. of unique reflections	35374
Redundancy	11.84 (11.96)
Completeness (%)	99.5 (99.6)
$I/\sigma(I)$	18.5 (7.9)
R_{merge} (%)	6.4 (27.2)
Ramachandran plot	
Core angles (%)	89.6
Additional allowed angles (%)	9.5
Generous allowed angles (%)	0.9
Disallowed angles (%)	0
Refinement statistics	
Completeness for range (%)	99.45
Reflections used for refinement	33575
Reflections used for R_{free} calculations	1770 (5%)
Crystallographic R (%)	20.3
R_{free} (%)	23.1
No. of protein atoms/average B-factor (Å^2)	1636/18.7
No. of inhibitor atoms/average B-factor (Å^2)	374/24.5
No. of sugar atoms/average B-factor (Å^2)	48/25.9
RMS deviations from ideal geometry	
Bond distances (Å)	0.011
Bond angles (°)	1.268

3. Results and discussions

3.1. Crystal structure of HNE and 1/2SLPI complex

Fig. 1(*a*) shows the complex structure of HNE and 1/2SLPI. In the contact region there are no covalent bonds between HNE and 1/2SLPI. The main-chain trace of HNE shows no differences from PDB (Protein Data Bank) id 1B0F (Cregge *et al.*, 1998). 1/2SLPI consists of four anti-parallel strands (strand from A to D) and four disulfide bridges (Cys64i–Cys93i, Cys71i–Cys97i, Cys80i–Cys92i, Cys86i–Cys101i), which keep the shape of 1/2SLPI like a rigid wedge.

Table 2
Inhibition constant (K_i values) of elafin (Zani *et al.*, 2004) and 50% inhibitory concentrations (IC50) of 1/2SLPI and against some serine proteases (Masuda *et al.*, 1994).

	K_i (M) of elafin	IC50 of 1/2SLPI
	57 amino acids A1–G57 42% identity with 1/2SLPI	49 amino acids R58–A107 C-terminal domain of SLPI
H. neutrophil elastase	1×10^{-10}	1.3×10^{-8}
P. pancreatic elastase	1×10^{-9}	3.3×10^{-5}
H. cathepsin G	–	8.0×10^{-9}
B. pancreatic chymotrypsin	–	8.0×10^{-9}
B. pancreas trypsin	–	2.0×10^{-6}

There are a small number of intra-hydrogen bonds and electrostatic interactions in the 1/2SLPI structure (Fig. 1*b*).

In these four strands, only two internal strands form a double-stranded twisted β-sheet (Lys91i–Gly95i and Gly98i–Val102i) connected by five main-chain–main-chain hydrogen bonds. These two strands are joined by a β-hairpin loop at Met96i–Cys97i. No main-chain–main-chain hydrogen bond is formed between the two parallel strands A and C, and one hydrogen bond is formed between strands B and D. In the region between the long loop AB and the adjacent hairpin loop CD, only one hydrogen bond is formed, connecting N of Cys71i and O of Met96i.

1/2SLPI has almost the same structure as the C-terminal domain of the full SLPI structure (W. Bode, private communication), with the root-mean-square deviation (RMSD) of the backbone atoms being 1.04 Å for residues Arg58i–Ala107i. The AB loop (between strands A and B) of 1/2SLPI binding to the active site of HNE has no serious affect on the enzyme structure. Both 1/2SLPI and elafin have four disulfide bridges at the same positions. The sequence identity is 42%; however, the P1-residue of elafin is Ala24i. The main-chain structures of the AB loop of both 1/2SLPI and elafin are similar. The AB loop of elafin should have a large flexibility, like 1/2SLPI (unpublished NMR data).

The primary interaction appears to be the P1-residue Leu72i, located in the S1 pocket, and the carbonyl oxygen accommodated in the oxyanion hole. 1/2SLPI:HNE has almost similar hydrogen bonds

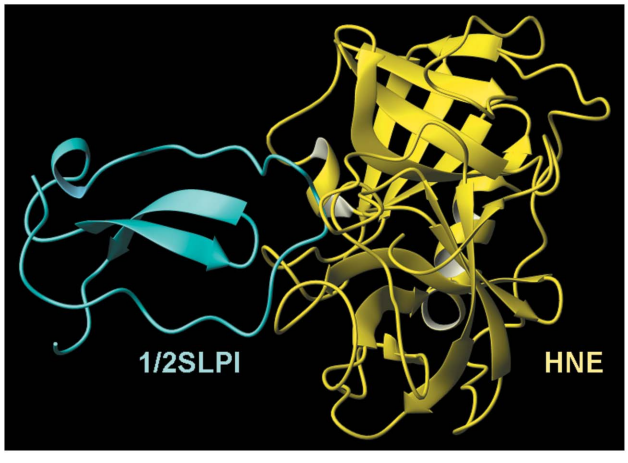

(*a*)

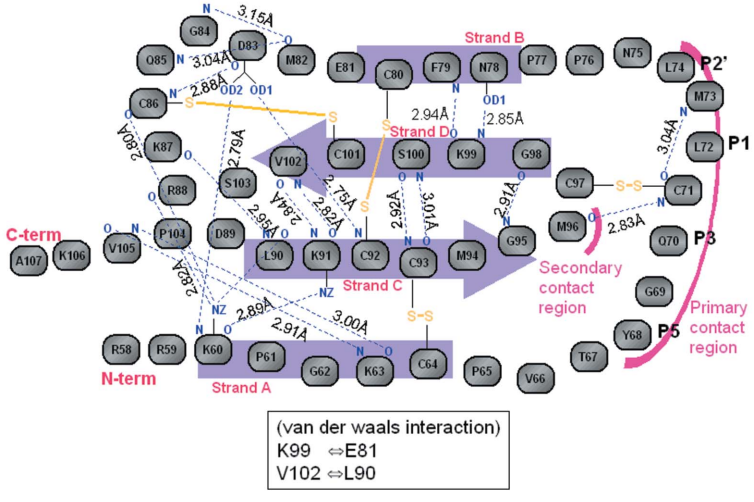

(*b*)

Figure 1
(*a*) The structure of the HNE and 1/2SLPI complex. The Cα linkage of 1/2SLPI is shown in blue and the Cα linkage of HNE is in yellow. (*b*) Schematic representation of the polypeptide chain folding of 1/2SLPI with its disulfide connectivities. Disulfide bonds are indicated by thin lines. The blue arrows show the twisted β-sheet (strands C, D), and the blue rectangles show the strands (strand A, B). AB and CD loops are shown by pink lines. Intramolecular hydrogen bonds are indicated by dashed lines, with distances shown. Intramolecular van der Waals interactions are also indicated at the bottom of the figure.

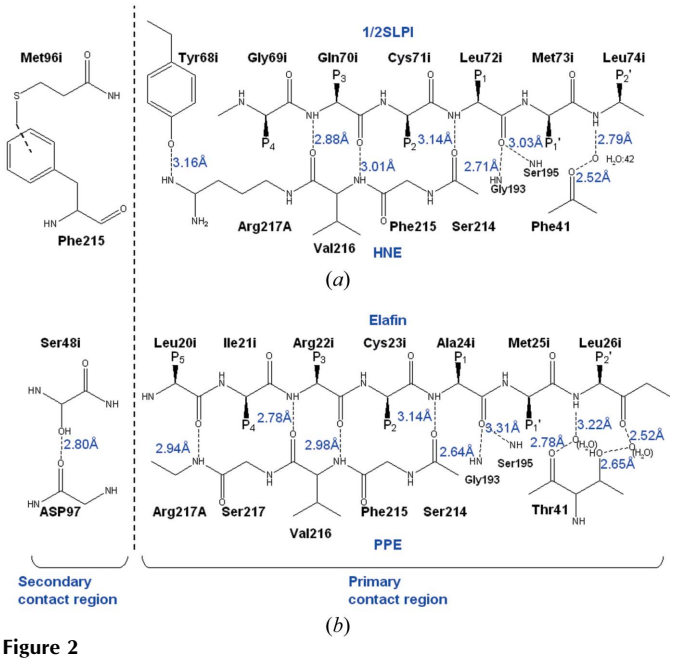

Figure 2
Schematic representation of the hydrogen-bonding interactions between the contact regions of (*a*) HNE and 1/2SLPI and (*b*) PPE and elafin (Tsunemi *et al.*, 1996). Inhibitor residues are designated by 'i' after the sequence number. Intermolecular hydrogen bonds are indicated by dashed lines.

at P2′–P3 in the primary contact site as elafin:PPE. Another hydrogen bond, Tyr68i(OH)···Arg217A(Nε1), in the primary contact region is added (Fig. 2*a*). Met96i (CD loop) is located near Phe215 with a longer distance than the usual van der Waals contact in the secondary contact region.

On the other hand, elafin has additional hydrogen bonds between the carbonyl oxygen of Leu20i (P5) and the main-chain NH of Arg217A in the primary contact region, and between the hydroxyl group of Ser48i and the carbonyl oxygen of Asp97 shown in Fig. 2(*b*) (Tsunemi *et al.*, 1996). The RMSD of the backbone atoms between 1/2SLPI and elafin is 1.01 Å, calculated by superposing residues Arg59i–Val105i of 1/2SLPI onto Thr11i–Gln57i of elafin. As shown in Table 2, 1/2SLPI shows a wide range of inhibitory activity against some serine proteases. On the other hand, elafin is a potent and specific protein inhibitor of PPE and HNE.

3.2. Difference in the inhibitory mechanism for elastases between elafin and 1/2SLPI

1/2SLPI:HNE has a similar interaction mode at P2′–P3 in the primary contact region as elafin:PPE. Figs. 3(*a*) and 3(*b*) show the S1 pocket of 1/2SLPI:HNE and elafin:PPE, respectively. They show that elafin does not fill the S1 pocket in the elafin:PPE complex structure and that SLPI fills the S1 pocket of HNE better. Leu72i (P1) of 1/2SLPI provides a large contribution in the recognition with HNE and PPE (Eisenberg *et al.*, 1990). Fig. 3(*c*) shows PPE superposing onto 1/2SLPI:HNE; the S1 pocket of PPE is similar to those of HNE. 1/2SLPI should show the same inhibitory activity against PPE on the S1 pocket, but 1/2SLPI inhibits HNE more than PPE (Table 2).

To understand 1/2SLPI's selectivity for HNE, we compared the interface of HNE and PPE around P5 and found a remarkable difference in these structures (Fig. 3). In the PPE's binding interfaces, Tyr68i (P5) conflicts with a region (Ser169–Val176) of PPE (shown in Figs. 3*d* and 3*e*). Tyr68i may be flipping away to avoid the conflict and cannot interact with PPE. In the 1/2SLPI:HNE complex, 1/2SLPI requires at least six hydrogen bonds between the main chains at P2′–P3 for the inhibitory activity owing to Leu72i (P1) occupation in the S1 pocket. Then the additional interactions at Tyr68i (P5) are used to increase the inhibitory activity of 1/2SLPI against HNE, but the interaction of the second contact region is not so critical.

On the other hand, elafin needs a full set of hydrogen-bonding interactions (seven hydrogen bonds of the main chain in the primary contact region and one in the secondary contact region) which should be essential for the inhibitory activity because Ala24i (P1) is insufficient in occupying the S1 site. The interacting mode of elafin:PPE may be kept in the elafin:HNE complex structure. It seems that the P1 and P5 residues of 1/2SLPI are important residues causing the selectivity against HNE.

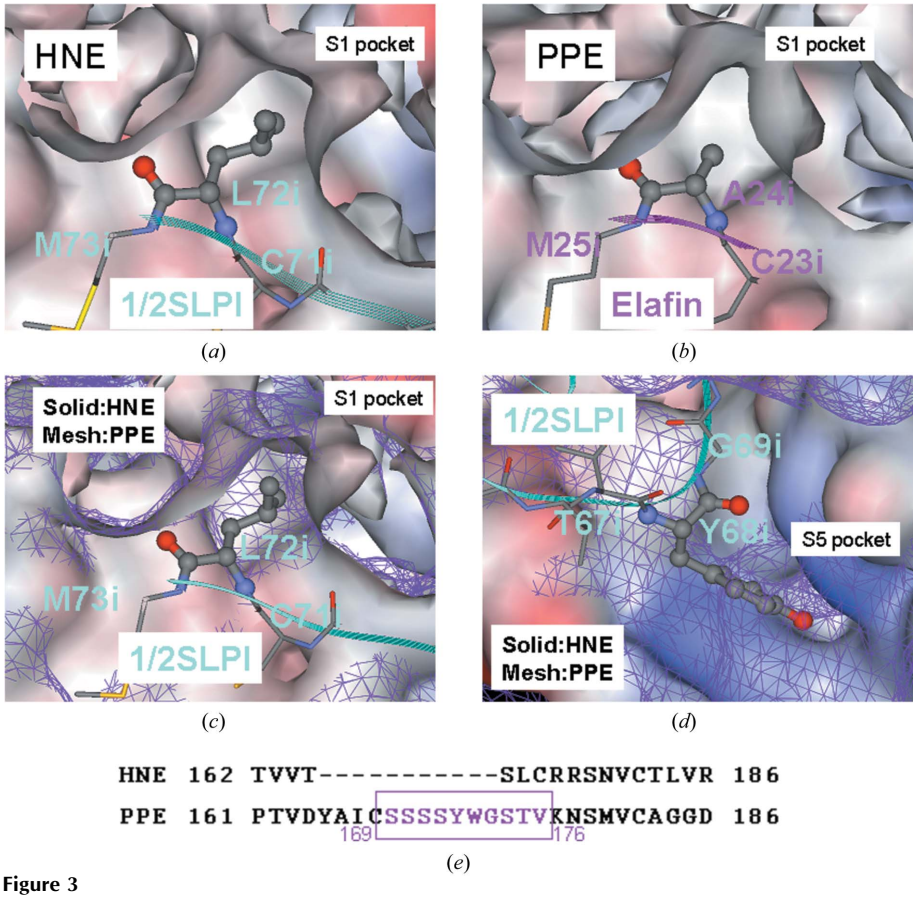

Figure 3
Electrostatic surface representations of (*a*) the HNE complex with 1/2SLPI (ball and stick model), and (*b*) the PPE:elafin complex around the S1 pocket. Superposed representations of the PPE molecule onto HNE of the X-ray structure HNE:1/2SLPI. The solid surface shows HNE and the meshed surface shows PPE. Comparison of HNE and PPE (purple mesh) around (*c*) the S1 pocket and (*d*) the S5 pocket. (*e*) The sequence alignment between HNE and PPE around the S5 pocket. The conflict residues of PPE with Y68i are shown in the purple square.

4. Conclusion

The current study shows the interaction mode between 1/2SLPI and HNE and it is similar to the elafin:PPE interaction modes. Although elafin inhibits both HNE and PPE equally, 1/2SLPI prefers HNE to PPE. We found that there were two important structural mechanisms which explained the selectivity of 1/2SLPI. First, the sufficient inhibitory activity of 1/2SLPI consists of six hydrogen bonds between the main chains at P2′–P3, owing to P1 (Leu72i) occupation of the S1 pocket. Second, additional interaction at P5 (Tyr68i) is possible in HNE, but impossible in PPE. P1 and P5 are critical residues for the selectivity of 1/2SLPI against HNE.

These recognition mechanisms for HNE may provide important information for understanding the multiple function of 1/2SLPI. To understand the versatility of 1/2SLPI against other serine proteases (chymotrypsin, trypsin, cathepsin *etc.*), we need additional structural information involving the structure determination of some other serine protease complexes with 1/2SLPI.

The crystal structure coordinates have been deposited with the Protein Data Bank (code 2Z7F).

We thank Dr Wolfram Bode (Max-Planck -Institute für Biochimie) for the coordinates of full SLPI.

References

Cregge, R. J. *et al.* (1998). *J. Med. Chem.* **41**, 2461–2480.
Eisenberg, S. P., Hale, K. K., Heimdal, P. & Thompson, R. C. (1990). *J. Biol. Chem.* **265**, 7976–7981.
Grütter, M. G., Fendrich, G., Huber, R. & Bode, W. (1988). *EMBO J.* **7**, 345–351.
Masuda, K., Suga, T., Takeuchi, A., Kanesaki, M., Imaizumi, A. & Suzuki, Y. (1994). *Biochem. Pharmacol.* **48**, 651–657.
Tsunemi, M., Matsuura, Y., Sakakibara, S. & Katsube, Y. (1996). *Biochemistry*, **35**, 11570–11576.
Wiedow, O., Luademann, J. & Utecht, B. (1991). *Biochem. Biophys. Res. Commun.* **174**, 6–10.
Wiedow, O., Schroder, J. M., Gregory, H., Young, J. A. & Christophers, E. (1990). *J. Biol. Chem.* **265**, 14791–14795.
Williams, S. E., Brown, T. I., Roghanian, A. & Sallenave, J. M. (2006). *Clin. Sci. (London)*, **110**, 21–35.
Zani, M. L., Nobar, S. M., Lacour, S. A., Lemoine, S., Boudier, C., Bieth, J. G. & Moreau, T. (2004). *Eur. J. Biochem.* **271**, 2370–2378.